NASA TECHNICAL NOTE

NASA TN D-5439

C. 1

NASA TN D-5439

FINAL REPORT: SATURN V, S-IVB PANEL FLUTTER QUALIFICATION TEST

by J. J. Nichols

George C. Marshall Space Flight Center
Marshall, Ala.

NATIONAL AERONAUTICS AND SPACE ADMINISTRATION • WASHINGTON, D. C. • OCTOBER 1969

FINAL REPORT: SATURN V, S-IVB PANEL FLUTTER QUALIFICATION TEST

By J. J. Nichols

George C. Marshall Space Flight Center
Marshall, Ala.

NATIONAL AERONAUTICS AND SPACE ADMINISTRATION

For sale by the Clearinghouse for Federal Scientific and Technical Information
Springfield, Virginia 22151 – Price $3.00

TABLE OF CONTENTS

LIST OF ILLUSTRATIONS

LIST OF TABLES

FINAL REPORT: SATURN V, S-IVB PANEL FLUTTER QUALIFICATION TEST

SUMMARY

This report gives results obtained from an evaluation of data taken during the Saturn S-IVB forward skirt flutter test conducted at Arnold Engineering Development Center, Tullahoma, Tennessee, during the period from October 30 through November 6, 1967. A fullscale segment of the S-IVB stage forward skirt was tested to determine the flutter characteristics of the thin skin panels bounded by internal rings and external stiffeners. The wind tunnel tests were conducted over a Mach number range of 1.3 through 1.6 and dynamic pressures to 950 psf.

Test runs were made by setting tunnel conditions shown in Table I and varying the compressive load on the specimen from 0 to 60 kips. Runs were also made at zero load while holding a constant Mach number and differential pressure across the specimen and varying the dynamic pressure. No flutter was noted during the dynamic pressure sweeps at zero axial load. Limited amplitude flutter was observed during most of the load sweeps. However, an inspection of the skirt segment did not reveal any noticeable damage such as cracks near the rivet lines resulting from the stresses induced by the flutter motion.

TABLE I. FLUTTER TESTS CONDUCTED

Mach Number	Dynamic Pressure psf	ΔP psi	Load kips
1.3	340 - 940	0.5	0.0
1.4	520 - 950	0.0	0.0
1.6	510 - 800	0.0	0.0
1.3	520, 940	0.5	0.0 - 60
1.4	320, 520, 740, 950	0.5	0.0 - 50
1.5	345, 520, 780, 860	0.5	0.0 - 60
1.6	340, 510, 800	0.0, 0.5	0.0 - 60

The test was terminated after a stringer located on the side of the test segment buckled under the applied compressive load. The stringer buckle originated across a permanent buckle in the adjacent skin that was "built-in" during fabrication of the specimen. The buckle occurred about five inches from the aft end of the specimen.

Since the skin panels were subjected to more severe flutter conditions than would be expected during flight, it is concluded that the S-IVB stage panel flutter is not critical for all Saturn IB and Saturn V published flight trajectories.

INTRODUCTION

During the flight trajectory of the Saturn vehicles, the thin skin panels in the S-IVB forward skirt are allowed to buckle since the stringers carry the flight loads in that area. This condition alters the panel stiffness and makes the panels more susceptible to flutter over a bounded load range. A limited-amplitude type of flutter may be tolerated during flight, provided the flutter amplitude and duration are such that structural failure caused by fatigue is not expected to occur. However, panel flutter of a catastrophic nature (rapid divergence type) must be avoided. The purpose of this test program was to experimentally qualify the forward skirt and to determine the flutter characteristics of the Saturn/S-IVB stage panels by subjecting a full-scaled model of a segment of the forward skirt to simulated flight conditions.

The tests were conducted in the Arnold Engineering Development Center (AEDC) 16-foot transonic wind tunnel. The tests described here are the second phase of flutter tests conducted at AEDC. The first phase was limited to a Mach number of 1.4 and a dynamic pressure of approximately 700 psf as a result of a wind tunnel compressor stage failure prior to the tests. Table I shows the flight conditions investigated during this second phase of testing. With full tunnel power available, a Mach number of 1.6 was attained. Test runs were made while holding the Mach number and dynamic pressure constant and varying the compressive load. The dynamic pressure was varied from 320 and 950 psf to provide a wide margin about the flight trajectory.

As stated above, the primary purpose of the tests were to qualify the S-IVB forward skirt for flight. Also of importance in evaluating future flights with similar skins is the effect of such parameters as stringer load or panel buckle amplitude, pressure differential, and dynamic pressure. General trends and limits of flutter as a function of these parameters are evaluated.

TEST SPECIMENS

Both a flutter model and a pressure survey model were used in the test program. The flutter model was a 30-degree segment of the S-IVB forward skirt. The skirt segment was constructed of 7075-T6 aluminum alloy consisting of internal rings, external hat-section longitudinal stringers mounted at 3 1/3 degree intervals, and a 0.032-inch skin. The skin was riveted to both the stringers and ring frames. This divided the test specimen into seven streamwise oriented arrays of five rectangular curved panels of various lengths. The model or test specimen was installed on a sealed mounting box which included a hydraulic loading system for applying compressive load to the specimen. The cavity depth behind the specimen was approximately 12 inches. The fixture consisted of a nose fairing of the same curvature as the S-IVB forward skirt, a boat tail and side struts which supported the assembled fixture in the tunnel as shown in Figure 1.

The test fixture was redesigned after the first test phase to eliminate undesirable wake effects on the turbine blades of the transonic wind tunnel at high dynamic pressures and Mach numbers. As a result of this redesign, it was necessary to repeat the Phase I pressure survey test to verify proper flow over the test specimen. The survey model was designed to simulate the external surface of the flutter model. The skin was constructed from a heavy gage steel to give a rigid panel surface from which to take measurements. Static pressure orifices were installed in the three center arrays of panels to measure the longitudinal pressure distribution. A rake of total pressure orifices was used to measure the boundary layer. The rake was mounted alternately at three positions along the centerline of the specimen. The pressure survey model was installed in the same test fixture as the flutter model.

INSTRUMENTATION

Pressure Survey Model

The pressure survey model imstrumentation consisted of static and total pressure orifices, oscillatory pressure microphones, and accelerometers, as shown in Figure 2. Static pressure orifices were located to define the longitudinal pressure distributions along three center arrays of panels. A rake of total pressure orifices was used to define the boundary layer. The rake was

mounted alternately at three positions along the length of the skirt segment. The oscillatory pressure microphones were used to measure the magnitude and the frequency content of fluctuating pressures on the specimen. Accelerometers were placed at each microphone location to measure vibration response.

The static and total pressure transducers were connected to an on-line digital computer system. Pressure coefficients along the length of the specimen and boundary layer profiles were monitored and photographed during the test on a graphical display unit connected to the on-line computer. Data printouts were also obtained. Raw signal data from the microphones and accelerometers were monitored on direct writing oscillographs and magnetic tape recorders.

Flutter Model

The flutter model was instrumented with uniaxial strain gages, oscillatory pressure microphones, and accelerometers, as shown in Figure 3. The strain gages, mounted on the under side of the specimen, were used to monitor panel flutter. Four microphones were mounted flush with the surface, on a center stiffener and another mounted on the floor of the pressure cavity. An accelerometer was mounted at each microphone to monitor vibration response of that point.

All transducers were monitored on direct writing oscillographs and also recorded on magnetic tape. The oscillographs were used to obtain quick look data, while the magnetic tape data served as input to a random vibration analysis for determining predominant frequencies and corresponding rms amplitudes in each signal.

A pressure cell was connected between a static pressure orifice, on the forward access panel, and the pressure cavity. This allowed continuous monitoring and control of the differential pressure across the test specimen.

TEST PROCEDURES

Pressure Phase

Static pressure distributions across the test specimen and boundary layer profiles were obtained at conditions listed in Table I. Data were obtained with the boundary layer rake alternately mounted in a forward, center, and aft position.

Flutter Phase

The Mach numbers of interest were first established at low dynamic pressures. Test runs were then made at zero axial load by varying the dynamic pressure while holding a constant ΔP pressure across the panel. Other runs were made while tunnel conditions were held constant and the test specimen loaded axially in compression from 0 to 60 kips. The dynamic pressures and ΔP's investigated are given in Table I. When the axial load reached 60 kips the ΔP pressure was increased to 2.0 psi to damp out or, in most cases, stop flutter. The load was then reduced to zero. The average time of a 0 to 60 kip load run was from about 40 to 50 seconds.

All oscillographs and tape recorders were on through the duration of each test run. Cameras were not turned on until several of the panels had begun to respond.

Five 16 mm movie cameras were used to photograph the panel response. Two cameras, with speeds of 400 and 1000 frames per second, were located above the panel. Three other cameras were mounted on the side of the tunnel at the forward end, center, and aft end of the panel. These cameras had speeds of 400, 1000, and 400 frames per second, respectively.

DISCUSSION

Static load tests conducted before the wind tunnel tests showed a variation in the compressive stress required to buckle the various skin panels. The reference load and compressive stress magnitude at which the three center arrays of panels bucked is given in Table II for varying differential pressure, ΔP. The center skin panels experienced pure compressive type buckles while the outside arrays showed the effects of side restraint and experienced a shear type buckle pattern. Panel stress levels were determined from three-axis rosette type strain gages mounted back-to-back on the inside and outside surfaces. In order to determine panel buckling, the compressive stress was plotted as a function of load applied to the specimen. Buckling was defined as the point where the panel stress did not increase with load. Figure 4 shows a photograph of the buckled skin panels under an applied load of 40 kips.

The objective of the test program was to qualify the S-IVB forward skirt by subjecting it to simulated flight conditions over the prescribed Mach

TABLE II. SKIN PANEL STATIC BUCKLING LOADS AND STRESSES

Panel	ΔP = 0 psi		ΔP = 0.5 psi		ΔP = 1.0 psi	
	Load kips	Stress psi	Load kips	Stress psi	Load kips	Stress psi
A-3	16.0	1250	20.0	2200	31	3300
A-4	–	–	17.0	1000	30	1800
A-5	15.0	500	17.0	700	29	1000
B-3	30.0	1900	33.0	2600	42	3550
B-4	10.0	750	23.0	1600	33	2700
B-5	24.0	2250	32.0	2500	43	3300
C-3	20.0	1700	30.0	3000	37	3400
C-4	9.0	500	23.0	1500	34	2500
C-5	14.0	700	21.0	1200	31	2300

number range. The stringers were loaded to stress levels above Saturn IB design limit stresses to assure that flutter in the wind tunnel occurred at skin panel buckle depths comparable to those experienced during flight. Table III shows a comparison of stringer stresses applied in the tunnel with stress levels measured during the S-IVB/Saturn IB 102 Percent Design Limit Loads test and maximum values measured during the AS-501 and AS-502 flights. It is seen that the panel was subjected to a more severe load condition in the tunnel than was experienced during Saturn V flights or at Saturn IB design limit load.

TABLE III. COMPARISON OF STRINGER STRESSES

Bay	Max Compressive Stress From Static Test on Flutter Specimen (psi)		Max Stress Saturn IB 102% Limit Load Test (psi)	AS-501 Flight Stress (psi)	AS-502 Flight Stress (psi)
	ΔP = 0	ΔP = 1.0 psi			
A	-12 200	-11 700	- 4 750		
C	-13 000	-11 000	- 8 800	-5 000[a]	-6 900[a]
D	-19 500[b]	-19 000[b]	-17 240		

a. Maximum compressive stress measured through 1.2-2.0 Mach no. range
b. Average value, peak compressive stress was 24 800 and 23 800 psi for ΔP = 0, and 1.0 psi, respectively. Load = 64 kips.

As a second consideration of panel loads, the buckle depth was measured during the static load test by moving deflection instruments along the skin surface of one panel at various load levels. The panel did not buckle instantaneously. Instead, the buckle depth grew gradually as load was applied. A maximum double amplitude buckle depth of 0.260 inch occurred at 60 kips compressive load with zero differential pressure across the panel. This compares with 0.244 inch deflection under 100 percent design limit load conditions as recorded during a S-IVB/Saturn IB buckling test in October 1965.

Pressure Survey Phase

Data from the pressure survey test showed that there were no flow irregularities over the model surface that might be detrimental to the flutter test results. Large positive pressure coefficients were observed near the aft end that resulted from flow separation caused by the aft ring frame and boat tail protruding into the air stream. The variation in pressure coefficient C_p with X/L at Mach numbers from 1.2 to 1.6 is presented in Reference 1. The high positive pressure coefficients occurred approximately 15 inches down stream from bay C where the nearest flutter was observed. It was concluded that the observed flutter was not affected by this pressure since the two regions were separated by a thick doubler and a ring frame as shown in Figure 3.

The boundary layer thickness varied from approximately 2.0 inches at the leading edge of the panel to 3.5 inches at the trailing edge. An increase of one inch in the boundary layer thickness was attained by placing a boundary layer trip along the leading edge of the test fixture. The measured boundary layer thickness was considerably less than the minimum predicted by the S-IVB stage contractor for flight conditions.

Flutter Phase

As previously described, two types of flutter tests were conducted. The first tests were conducted by varying the dynamic pressure while holding zero axial load and a constant ΔP pressure across the panel. These runs were made at the beginning of the test to assure that no flutter would be encountered while establishing tunnel conditions for the axial load runs. As expected, no flutter was observed during this test phase.

Limited amplitude flutter was observed during most of the axial load sweep tests at tunnel conditions listed in Table I. The general trend was for the flutter amplitude to increase as the applied load increased. In many cases the flutter amplitude peaked before the 60 kip load was reached and then either remained constant or decreased as loading continued. Other panels stopped fluttering as the load increased. Evidence of the above trends are shown by the strain gage traces in Figures 5 and 6 for several test conditions. Figure 5 shows the flutter amplitude history from beginning to end of several load sweeps while Figure 6 shows part of one run with a "blown up" time scale.

Other tests have shown that stressed panels have flutter boundaries that are dependent on their stress state as well as such parameters as Mach number, dynamic pressure, and geometry. The panel becomes more susceptible to flutter near its critical buckling stress and less susceptible as more load is applied and the buckle depth increases. A panel loaded in compression then has a bounded load region, above a given dynamic pressure, through which flutter would occur.

A flutter boundary was constructed in Figure 7 for several S-IVB skirt panels that stopped flutter during the M=1.6, $\Delta P=0$ load sweeps. The boundary consists of three parts. At lower loads, the panel is flat and the dynamic pressure required to cause flutter decreases with increasing load. The transition point, where the panel goes from a flat to a buckled state, is the lowest critical dynamic pressure on the boundary curve. Along the third and last part of the curve, the panel is buckled, and the dynamic pressure required for flutter increases with increasing load. The indicated transition point occurs at a much higher load than the no-flow buckling loads given in Table II. A review of the wind tunnel data showed that the load difference could not be attributed to an increase in differential pressure. An apparent increase in panel buckling strength when subjected to supersonic flow has been observed by other investigators [2, 3] at a Mach number of 3.0. The phenomena has also been supported theoretically.

It is well known that the flutter characteristics of a panel are very sensitive to its buckling characteristics as previously shown by the flutter boundary in Figure 7. In comparing the static buckling stresses in Table II, one observes that the panels which started and stopped flutter did have a lower buckling stress than panels that continued to respond through the entire load range. Since the stiffer panels would be expected to respond with characteristics similar to the less stiff ones, it may be concluded that all the panels would have stopped flutter if the required higher load had been applied to the specimen.

An analysis of the strain gage data was made to obtain the frequency content and corresponding rms amplitudes in the monitored flutter response. Table IV shows the results of this analysis along with maximum peak amplitudes of the signal. The results given were obtained from a one second time slice at the point where the raw data signal peaked. Unfortunately the strain gage that showed the maximum strain amplitude of the entire test could not be analyzed because of a bad calibration on the magnetic tape. This gage, located on panel C-3, showed $\pm 2500\ \mu$ in./in. strain on the on-line oscillograph at the tunnel condition M=1.6; q=510 psf; and $\Delta P = 0$.

As seen in the table, the general trend was for both the predominant response frequency and amplitude to increase as the dynamic pressure increased. Some panels had secondary frequencies with approximately the same response amplitude as the primary ones. Others responded at only one predominant frequency as indicated by the typical power spectral density plot in Figure 8.

Because of the type flutter observed, it can be concluded that failure of a panel would be of a fatigue nature and not of the catastrophic flutter nature as predicted by classical flutter theory. Figure 9 gives a comparison of AS-502 and 204 flight trajectories with data points obtained during the wind tunnel tests. The AS-502 trajectory (the most severe Saturn trajectory published to date) is below the maximum dynamic pressures attained throughout the tested Mach number range. The applied compressive stringer stresses were also comparable to those expected during future Saturn flights. Therefore, the data presented includes flutter amplitudes and frequencies which correspond to more severe conditions than is expected to occur during flight.

The tests were terminated after a side stringer on the specimen buckled under the applied compressive load. The stringer buckled across a permanent buckle in the adjacent skin that was "built-in" during fabrication. The skirt segment was a Saturn IB design, and, therefore, had to be heavily loaded to assure comparison of test to Saturn V skin buckle depths. The stringer buckle occurred about five inches from the aft end of the skirt segment. A photograph of this damaged area is shown in Figure 10.

TABLE IV. PREDOMINANT PANEL FREQUENCIES AND AMPLITUDES

Panel No.	Mach No.	P psi	q psf	Predominant Freqs.[a] and Corresponding Amp.[b]								c Peak Amp
				$Freq_1$	Amp_1	$Freq_2$	Amp_2	$Freq_3$	Amp_3	$Freq_4$	Amp_4	
A-3	1.4	0.5	950	285	1123	270	139	305	132	860	95	
	1.6	0.0	510	185	611	200	443	365	120	240	119	1450
	1.6	0.0	800	280	1087	560	137	335	68	255	66	1600
A-5	1.3	0.5	512	225	735	450	116	250	63	685	51	1400
	1.3	0.5	940	290	695	580	190	870	125	40	48	1200
	1.4	0.5	730	290	99	580	38	—	—	—	—	250
	1.4	0.5	950	330	672	290	427	655	348	985	193	2000
	1.5	0.5	860	320	708	285	397	645	388	965	232	2000
	1.6	0.0	340	240	730	475	168	715	122	220	70	1300
	1.6	0.0	510	290	827	315	107	580	51	—	—	1500
	1.6	0.0	800	335	1061	670	147	320	126	355	76	2000
B-2	1.4	0.5	950	295	309	460	119	355	116	390	115	1500
	1.5	0.5	860	290	205	305	180	330	142	420	129	
B-3	1.3	0.5	940	175	478	155	160	—	—	—	—	1100
	1.4	0.5	950	185	349	200	259	370	227	415	148	1300
	1.5	0.5	780	250	197	280	149	20	105	310	101	1400
	1.6	0.5	510	170	347	345	149	220	112	265	78	1200
	1.6	0.5	800	310	198	335	177	285	135	540	103	1400
	1.6	0.0	340	90	521	175	207	105	106	265	90	1100
	1.6	0.0	510	165	420	345	89	270	51	—	—	1800
	1.6	0.0	800	260	253	285	220	300	160	220	140	1850
B-4	1.3	0.5	940	175	591	105	158	135	90	235	88	1300
	1.4	0.5	950	185	349	200	259	370	227	415	148	1300
	1.5	0.5	515	160	316	145	185	15	112	30	106	1000
	1.5	0.5	780	290	253	305	218	260	211	325	139	1600
	1.5	0.5	860	305	285	275	235	335	145	355	104	1500
	1.6	0.5	510	225	213	190	183	170	137	270	126	1300
	1.6	0.5	800	330	273	355	150	370	141	390	132	1600
	1.6	0.0	340	95	175	125	173	25	121			700
	1.6	0.0	510	210	307	220	303	175	199	185	195	1400
	1.6	0.0	800	285	363	305	309	270	274	345	167	2000
B-5	1.3	0.5	940	175	467	150	74	125	54	—	—	1100
	1.4	0.5	730	160	288	330	73	—	—	—	—	900
	1.4	0.5	950	300	295	315	189	260	141	370	109	1500
	1.5	0.5	515	160	138	145	96	—	—	—	—	550
	1.5	0.5	780	260	181	310	167	295	167	335	138	1500
	1.5	0.5	860	275	225	290	203	315	170	345	136	1400
	1.6	0.5	510	140	258	125	252	85	116	—	—	1100
	1.6	0.5	800	310	217	285	200	330	173	345	133	1400
	1.6	0.0	510	205	158	220	132	235	126	65	111	1200
	1.6	0.0	800	275	340	260	273	225	163	305	155	1750
C-2	1.3	0.5	940	90	833	45	129	135	124	185	81	1650
	1.4	0.5	950	180	587	150	152	390	68	—	—	1750
	1.5	0.5	780	210	359	220	344	170	180	150	125	1600
	1.6	0.5	510	110	376	190	221	160	56	—	—	750
	1.6	0.5	800	240	306	480	156	290	100	190	90	1500
	1.6	0.0	340	65	315	80	260	100	112	120	108	1000
	1.6	0.0	510	120	342	140	211	240	113	225	100	1600
	1.6	0.0	800	220	363	165	84	285	66	440	64	1700
C-4	1.3	0.5	940	45	400	75	261	100	190	145	117	1700
	1.4	0.5	730	145	495	285	160	305	105	430	78	1300
	1.4	0.5	950	185	706	365	113	220	105	240	85	1900
	1.5	0.5	780	235	483	217	234	320	61	—	—	1650
	1.5	0.5	860	270	420	245	303	220	183	205	119	1750
	1.6	0.5	510	55	122	100	120	80	93	135	93	800
	1.6	0.5	860	255	442	185	97	315	78	555	76	1700
	1.6	0.0	510	135	461	160	270	170	256	105	193	1750
	1.6	0.0	800	235	470	265	190	195	118	470	105	1700

a. Frequency, Hz
b. Uniaxial Strain Gage rms Amplitudes, μin./in.
c. Peak Single Amplitude Obtained from Raw Data Plots μ in./in.

RESULTS AND CONCLUSIONS

The results of the pressure survey phase of the test were satisfactory. The data show that excellent flow conditions existed over the model with the exception of the aft portion of the skirt segment where high positive pressure coefficients were observed. It was concluded that the pressure did not affect the flutter results obtained since this area was well removed from where flutter was monitored. Also, there was no evidence in the microphone data of boundary layer fluctuations exciting the skin panels.

The panel flutter observed was of the limited amplitude type. Both the response amplitude and frequency increased with increasing dynamic pressure. During the compressive load sweeps the response increased with increasing load. It peaked on many panels before the maximum load was reached and either remained constant or decreased as loading continued. Some panels ceased to respond before the 60 kip load was reached. It can be reasoned that all the panels would have stopped flutter if a sufficient load had been applied.

Boundary layer effects lend some conservatism to the test because the wind tunnel model boundary layer thickness was less than predicted for flight.

A considerable amount of flutter time was accumulated for various panels as compared to the critical vehicle flight time. However, an inspection of the flutter model gave no indications of fatigue or overstressing problems.

Since the skin panels were subjected to more severe conditions than would be expected in flight, it is concluded that the S-IVB stage panel flutter has been proven not critical for all Saturn IB and Saturn V published flight trajectories.

George C. Marshall Space Flight Center
National Aeronautics and Space Administration
Marshall Space Flight Center, Alabama 35812
932-33-01-00-62

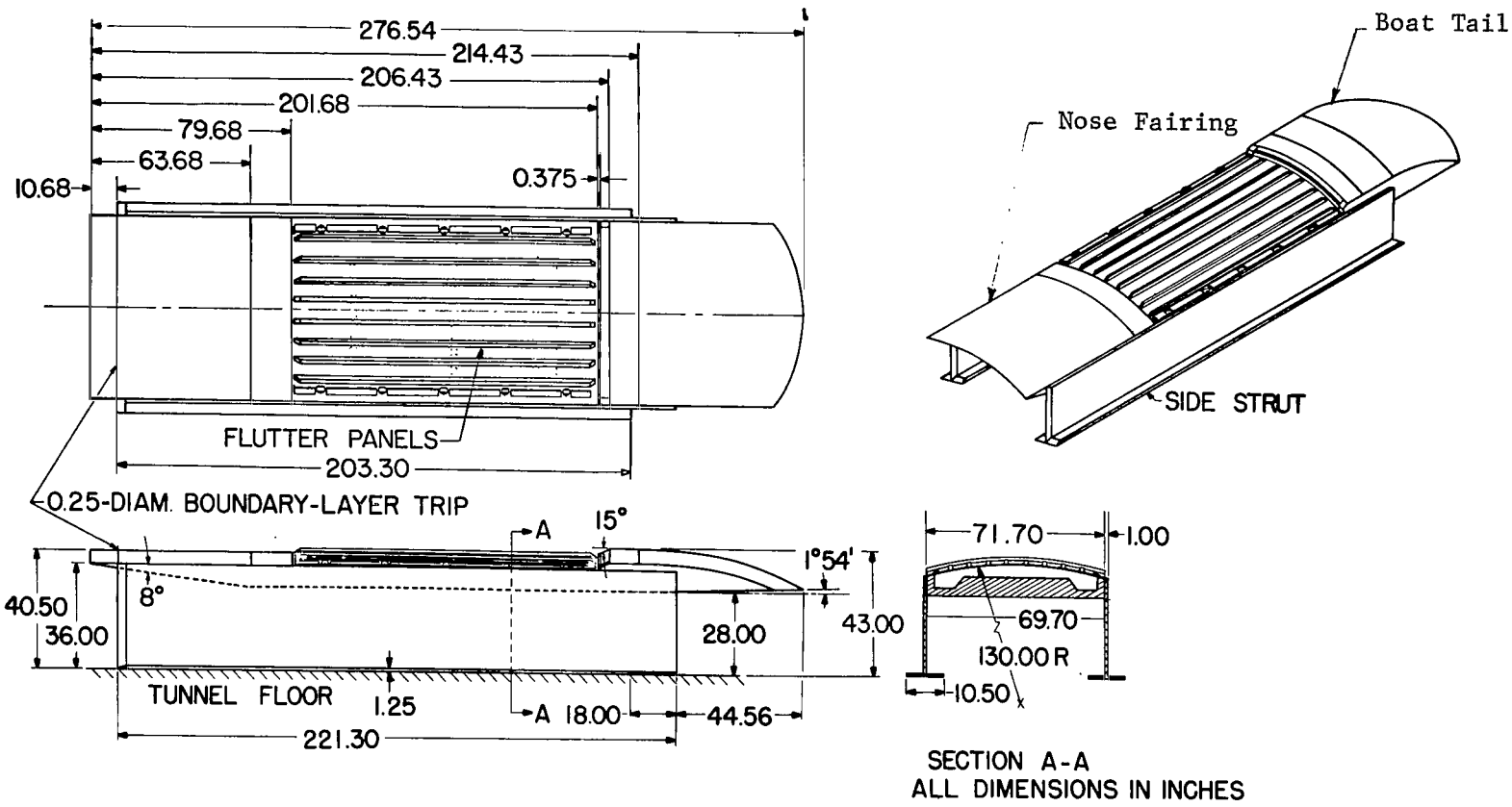

FIGURE 1. DETAILS OF TEST FIXTURE WITH FLUTTER PANEL INSTALLED

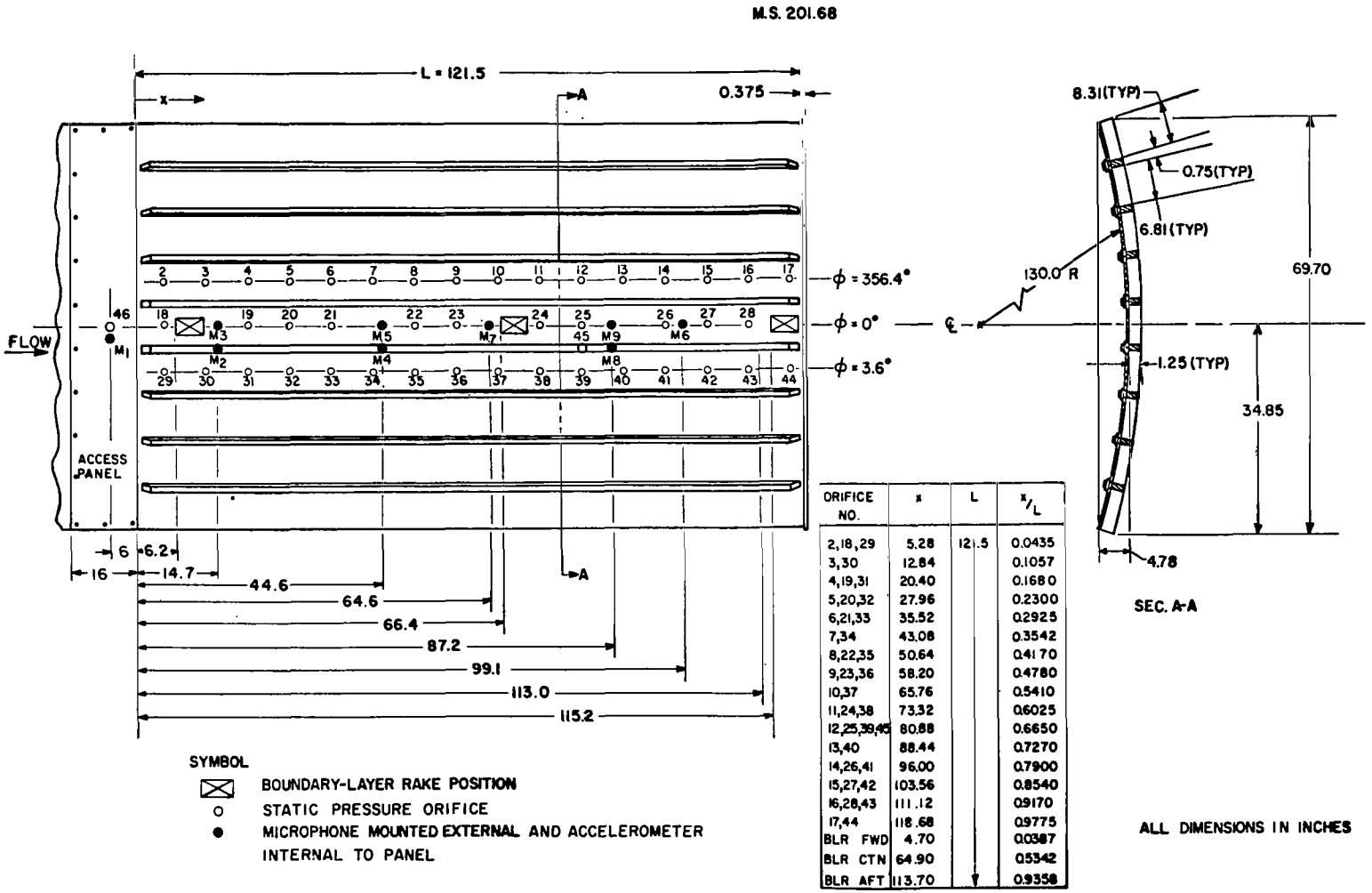

ORIFICE NO.	x	L	x/L
2,18,29	5.28	121.5	0.0435
3,30	12.84		0.1057
4,19,31	20.40		0.1680
5,20,32	27.96		0.2300
6,21,33	35.52		0.2925
7,34	43.08		0.3542
8,22,35	50.64		0.4170
9,23,36	58.20		0.4780
10,37	65.76		0.5410
11,24,38	73.32		0.6025
12,25,39,45	80.88		0.6650
13,40	88.44		0.7270
14,26,41	96.00		0.7900
15,27,42	103.56		0.8540
16,28,43	111.12		0.9170
17,44	118.68		0.9775
BLR FWD	4.70		0.0387
BLR CTN	64.90		0.5342
BLR AFT	113.70		0.9358

FIGURE 2. PRESSURE SURVEY PANEL

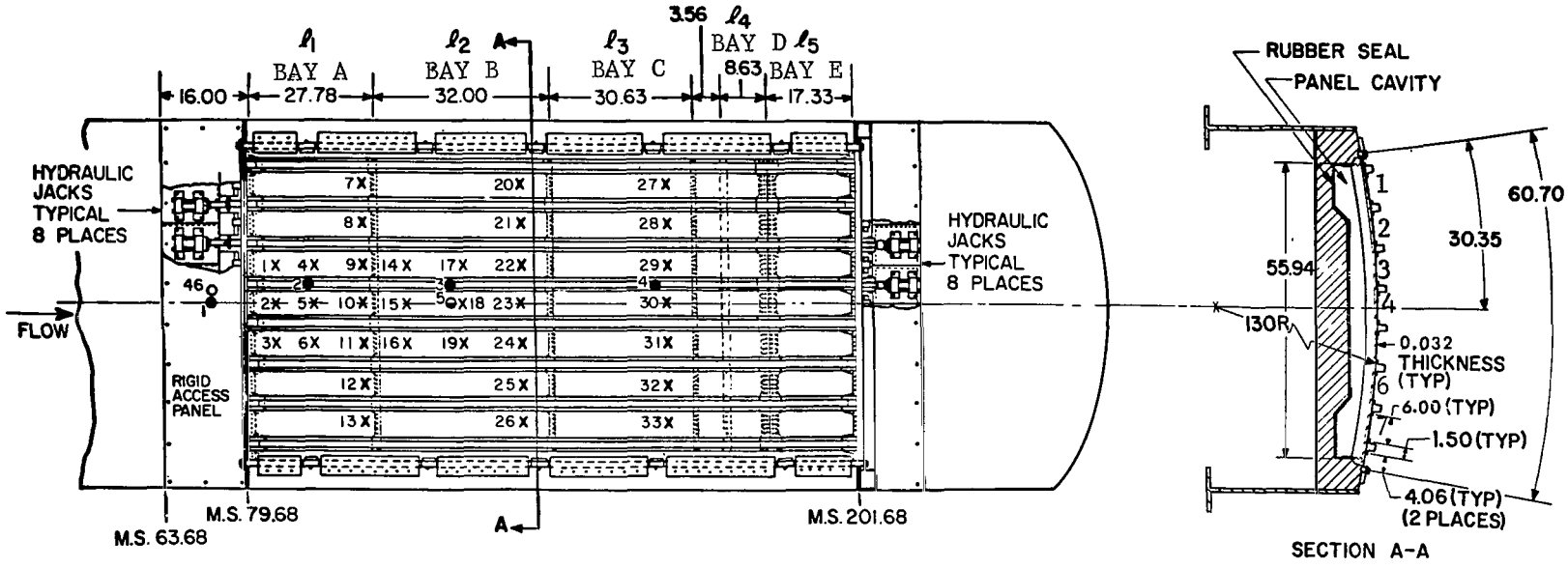

SYMBOL NUMBERS		LOCATION (M.S.)
STRAIN GAGES	ACCELEROMETERS AND MICROPHONES	
	1	73.68
1,2,3		83.62
4,5,6	2	90.57
7,8,9,10 11,12,13		100.46
14,15,16		112.46
17,18,19	3,5	120.46
20,21,22,23 24,25,26		132.46
27,28,29,30 31,32,33	4	163.09

SYMBOL

- o STATIC PRESSURE ORIFICE FOR p_{46}
- x STRAIN GAGE
- ● MICROPHONE MOUNTED EXTERNALLY AND ACCELEROMETER MOUNTED INTERNALLY TO PANEL
- ⊖ MICROPHONE MOUNTED INTERNALLY TO PANEL

ALL DIMENSIONS IN INCHES

FIGURE 3. FLUTTER PANEL

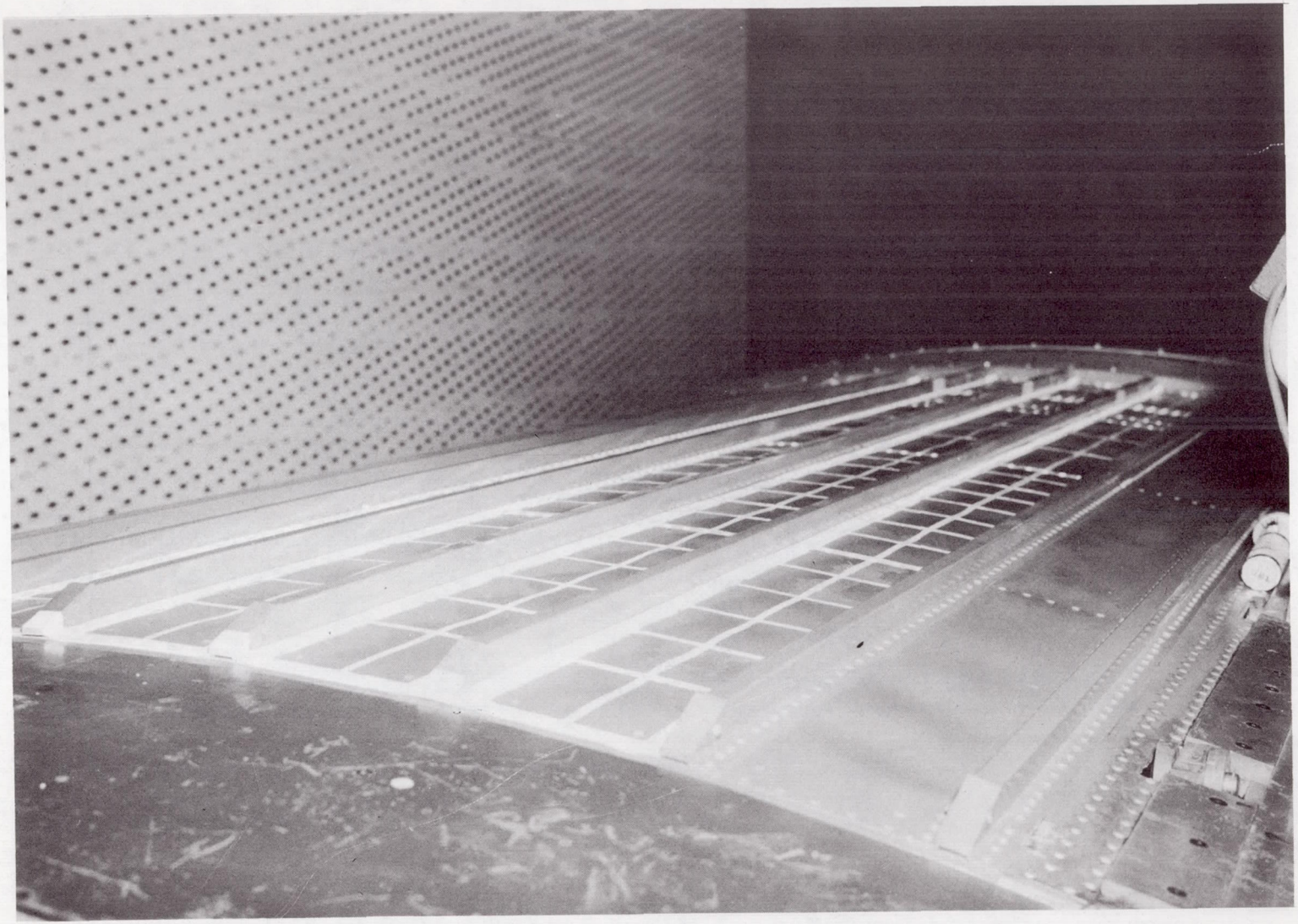

FIGURE 4. PHOTOGRAPH SHOWING SKIN BUCKLES AT 40 kips LOAD WITH NO FLOW

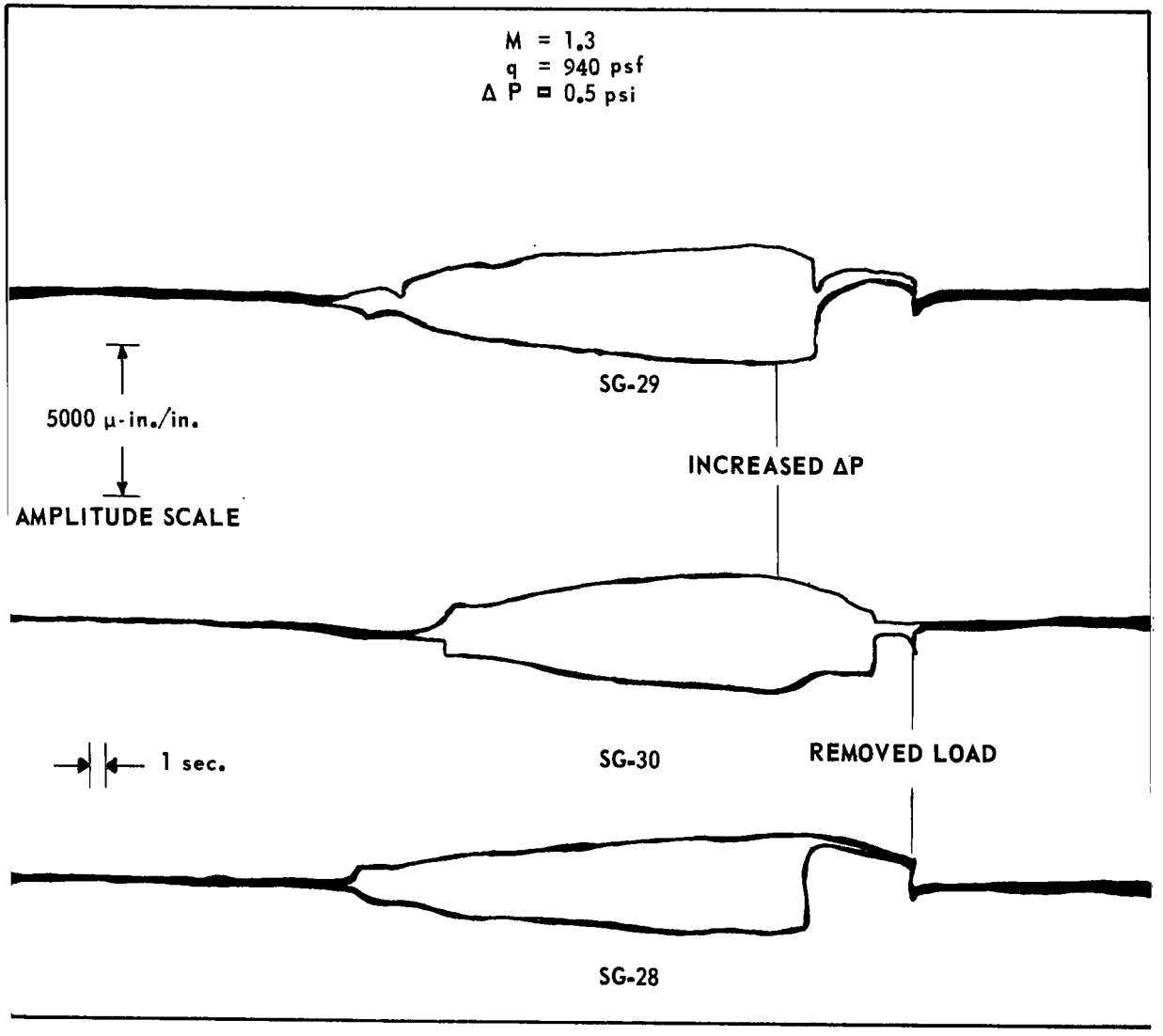

FIGURE 5. TYPICAL FLUTTER RESPONSE VERSUS COMPRESSIVE LOAD

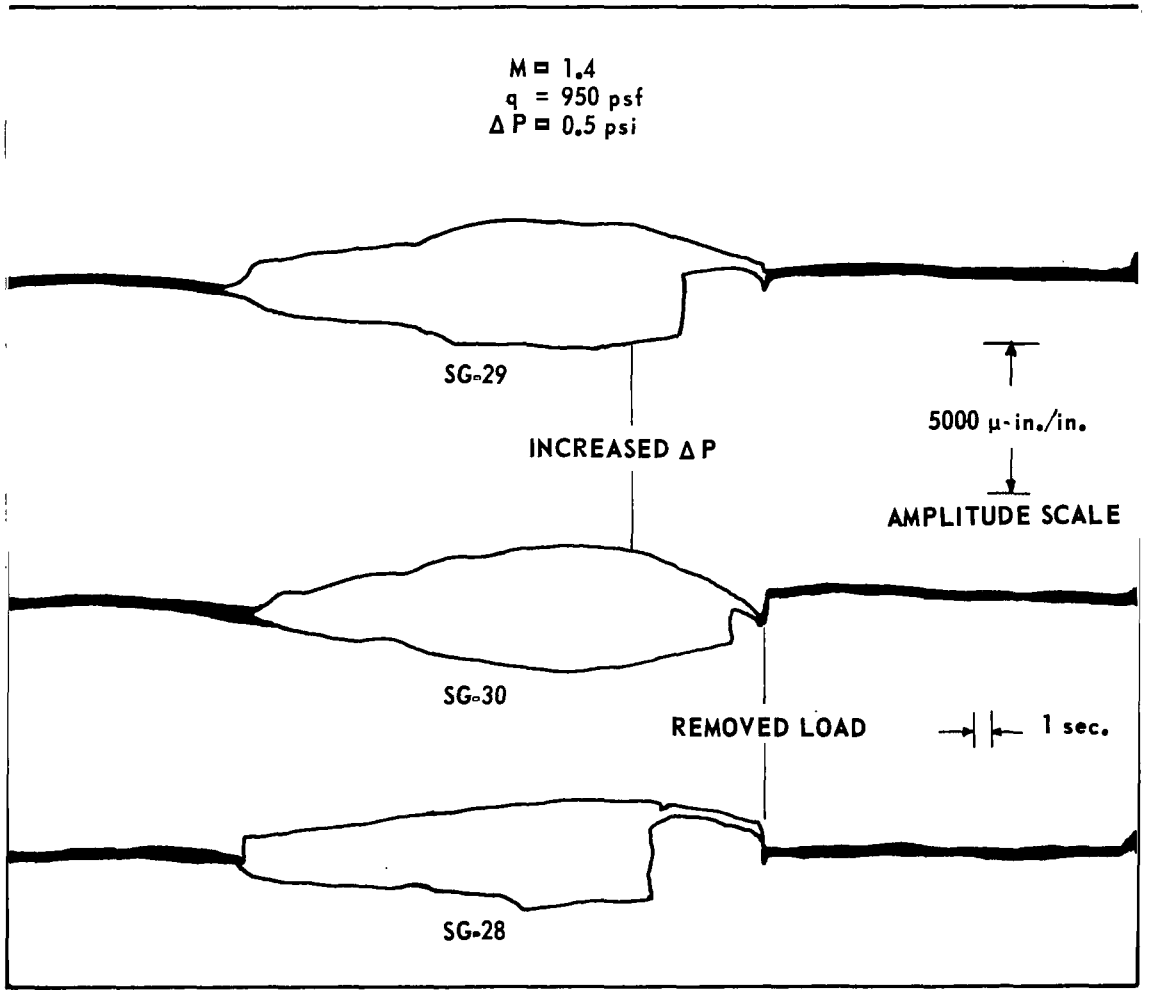

FIGURE 5. (Continued)

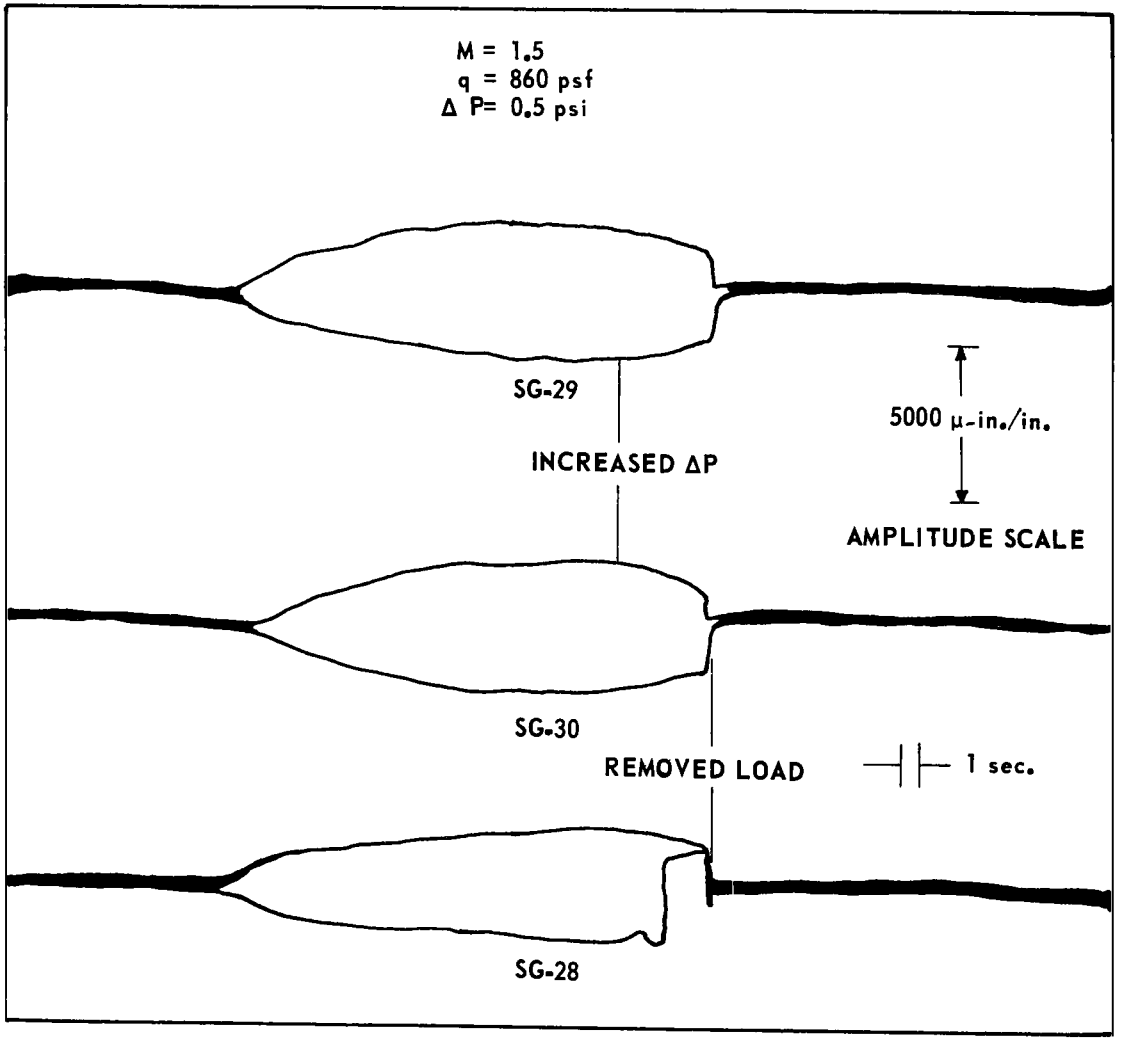

FIGURE 5. (Continued)

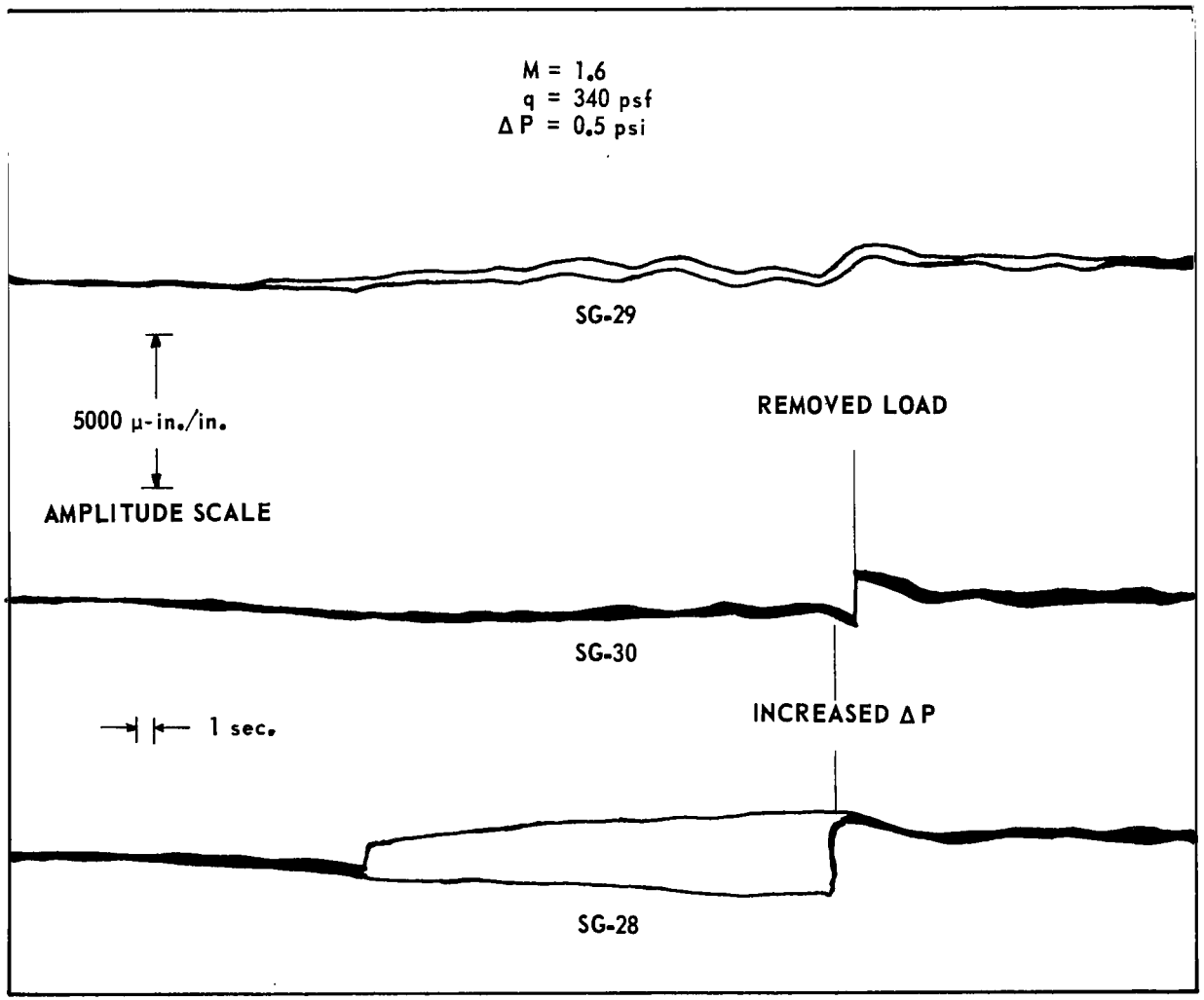

FIGURE 5. (Continued)

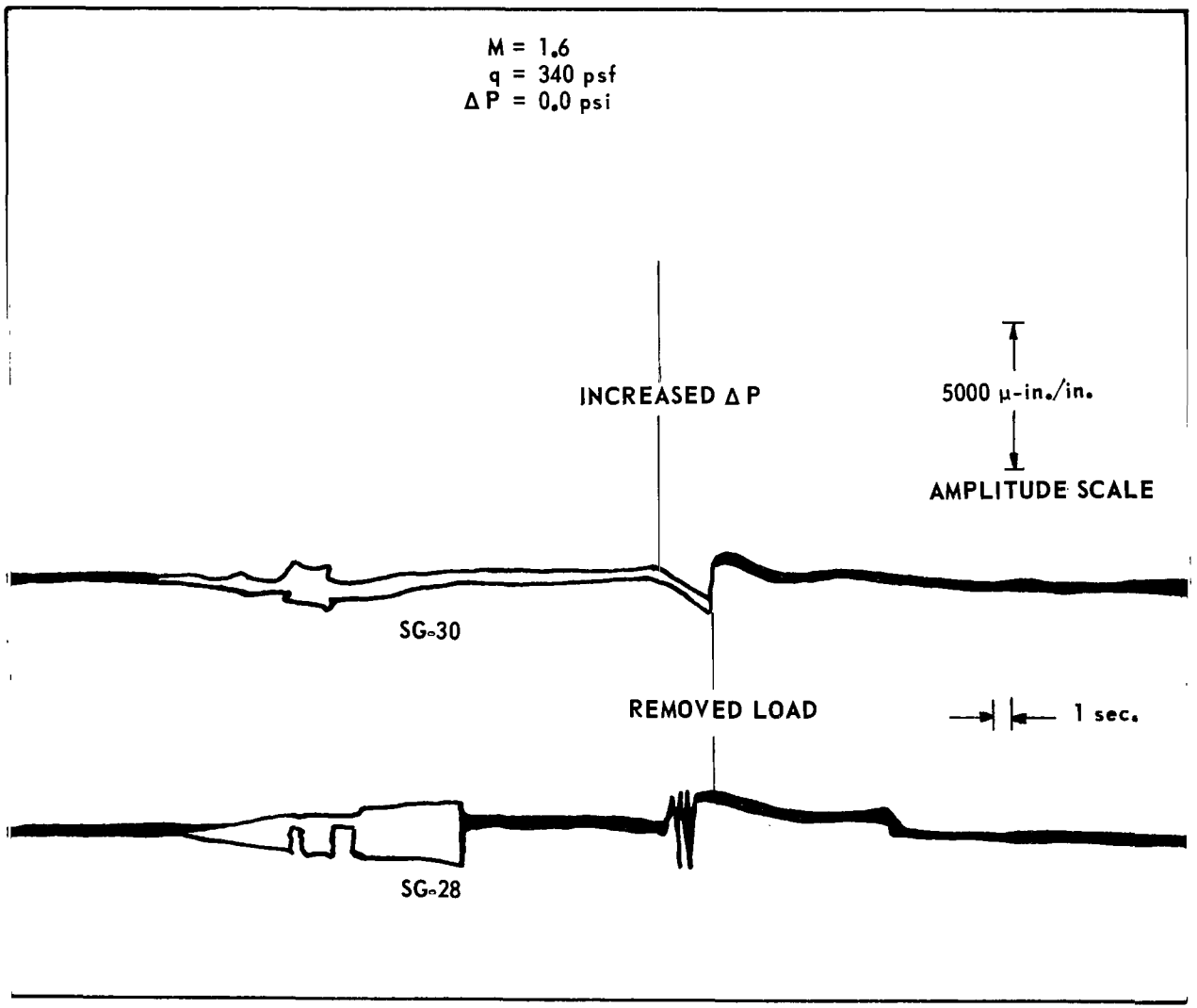

FIGURE 5. (Continued)

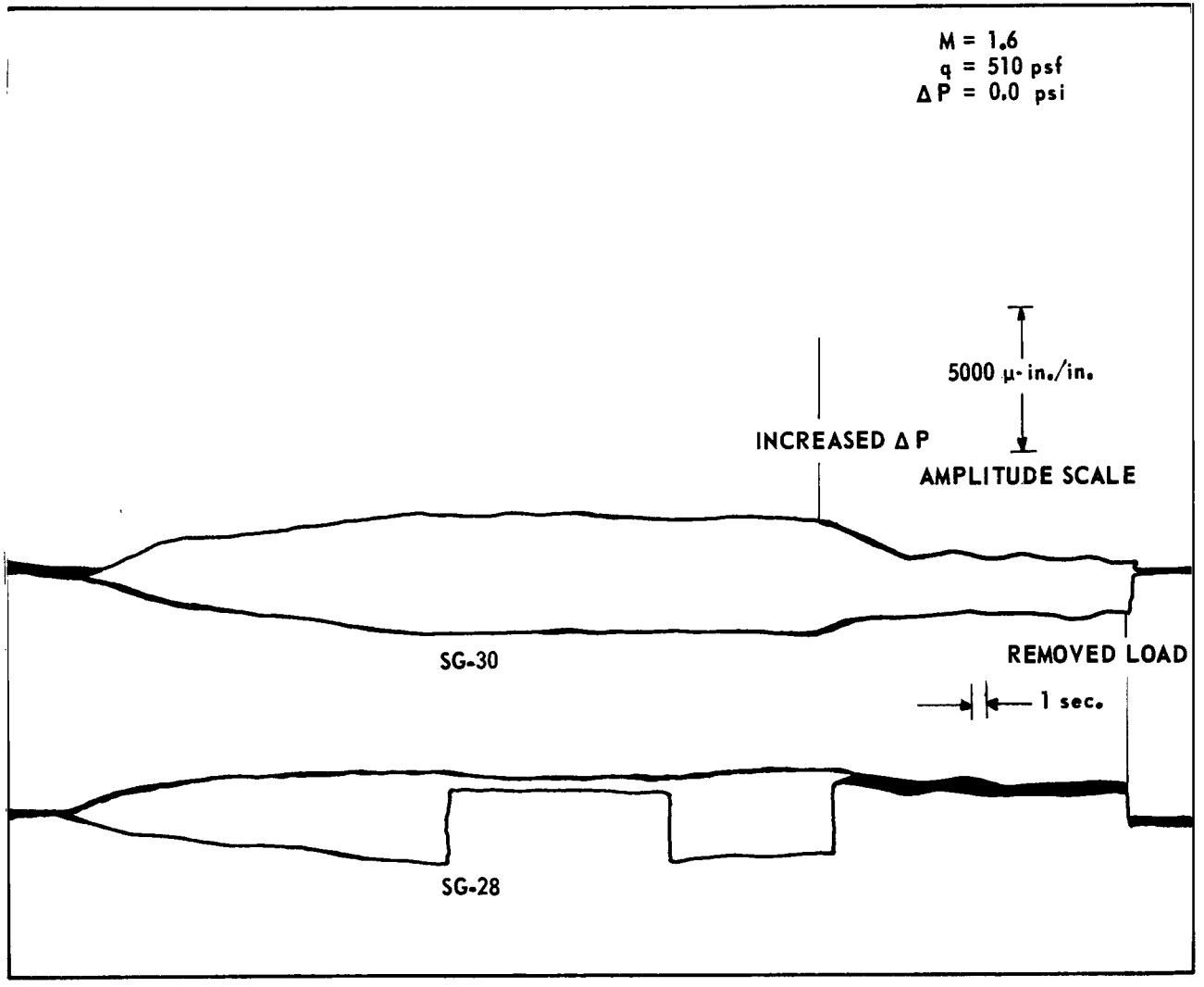

FIGURE 5. (Continued)

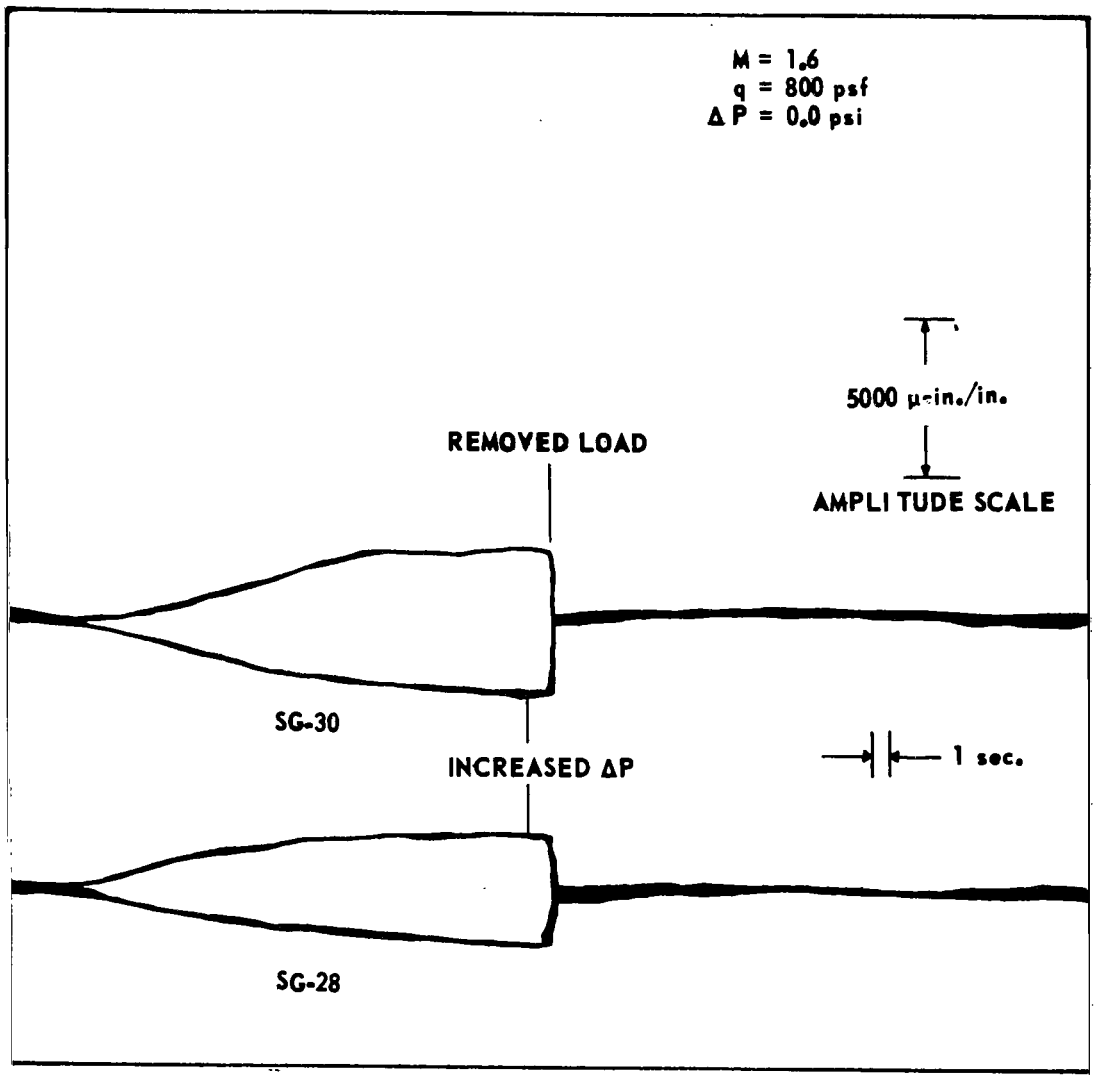

FIGURE 5. (Concluded)

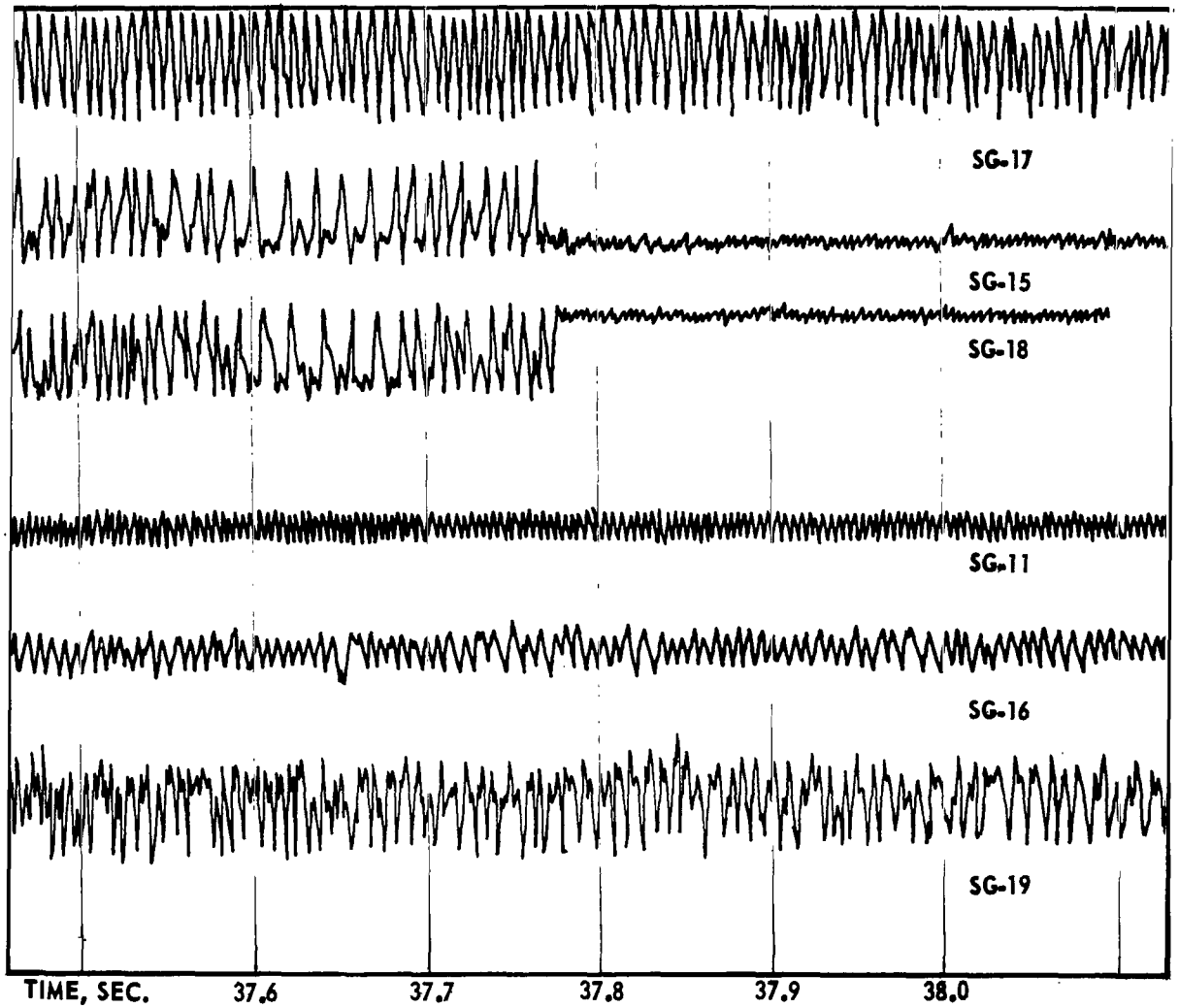

FIGURE 6. HIGH LOAD OSCILLOGRAPH TRACE
M=1.6; q=510 psf; P=0; Load=60 kips

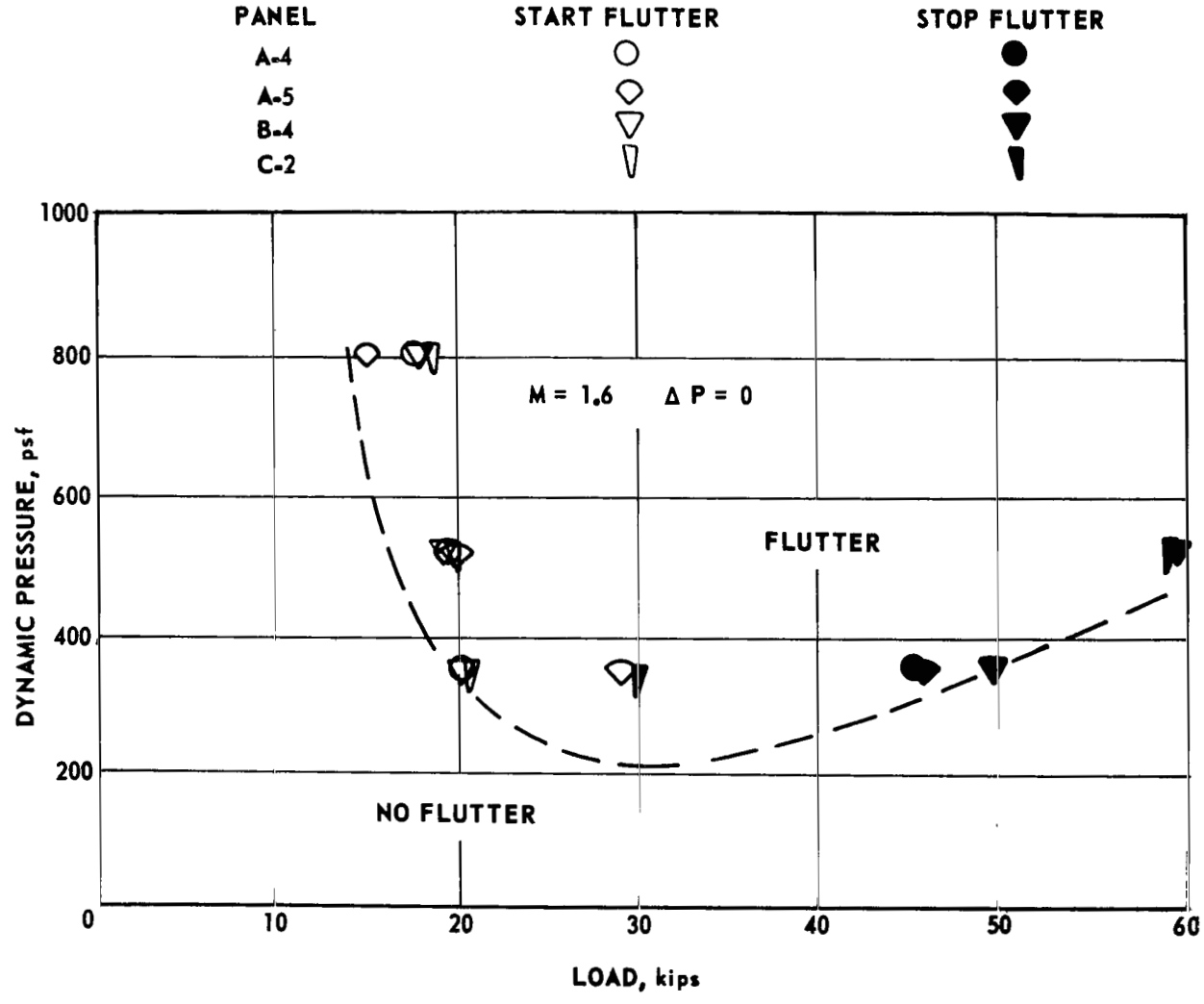

FIGURE 7. FLUTTER BOUNDARY

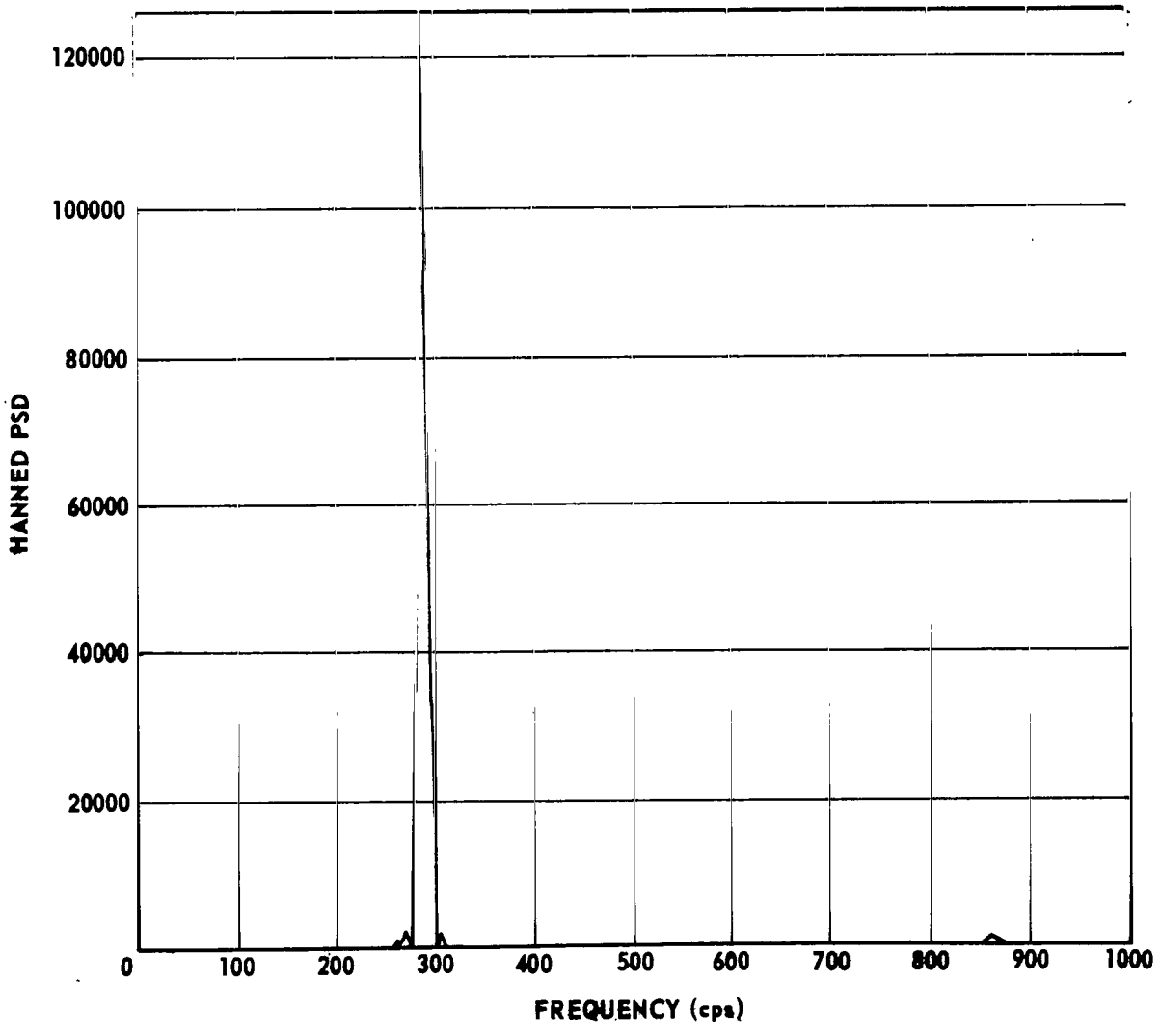

FIGURE 8. PSD PLOT FROM STRAIN GAGE ON PANEL A-3
(M=1.4; ΔP=0.5 psi; q=950 psf)

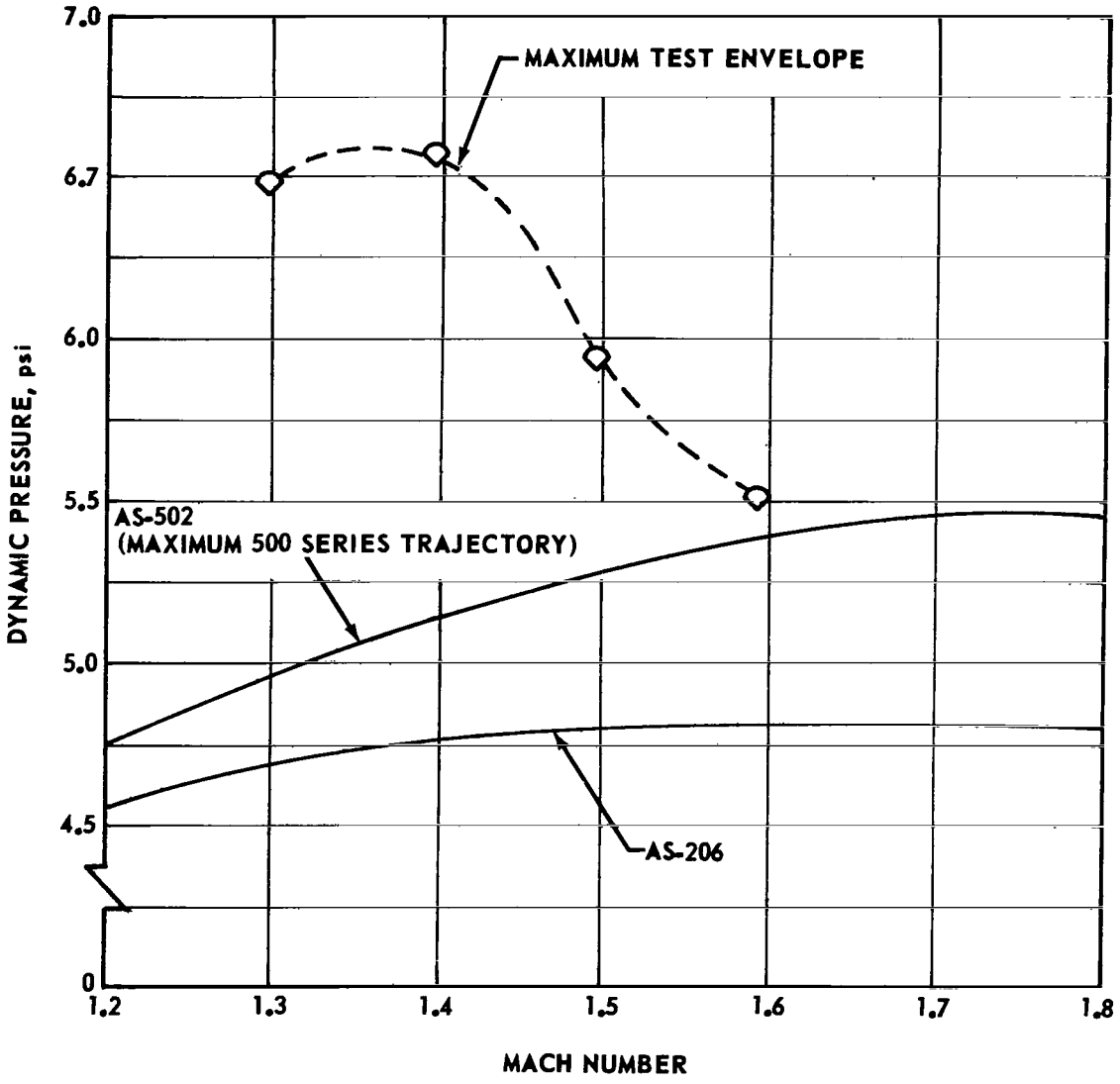

FIGURE 9. COMPARISON OF TEST AND FLIGHT ENVELOPES OF DYNAMIC PRESSURE VERSUS MACH NUMBER

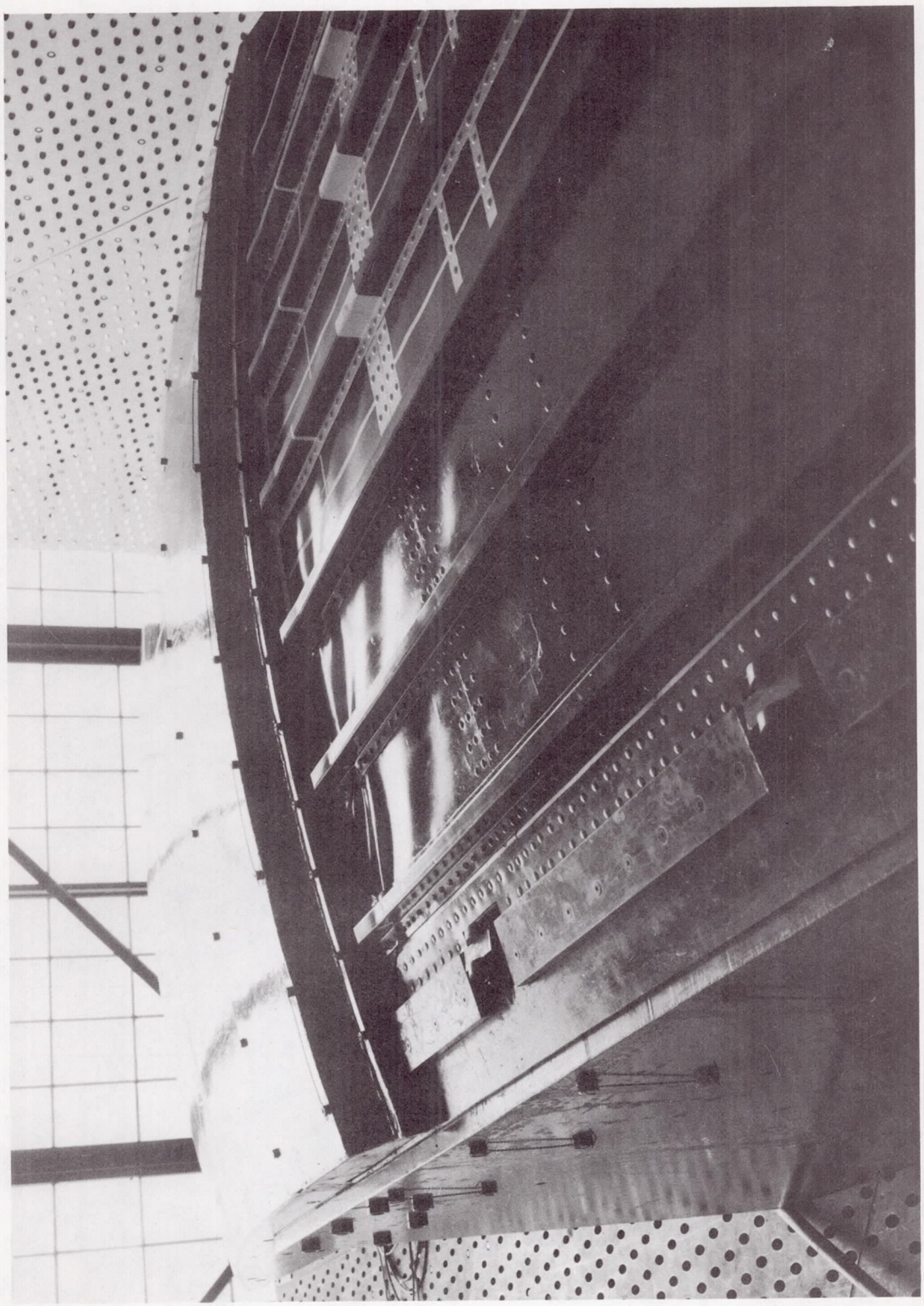

FIGURE 10. PHOTOGRAPH OF DAMAGED PANEL

MSFC—RSA, Ala

REFERENCES

1. Perkins, T. M.: Flutter Test of an Array of Full-scale Panels From the Saturn S-IVB Stage at Transonic Mach Numbers. Arnold Engineering Development Center, TR-68-30, February 1968.

2. Walker, Rosecrans, and Deveikes: Flutter Investigation of Streamwise Oriented Arrays of Curved Panels Under Compressive Loading and Aerodynamic Heating. NASA TN D-2910, July 1965.

3. Dixon, Sidney C.: Application of Transtability Concept to Flutter of Finite Panels and Experimental Results. NASA TN D-1948, 1963.

NASA-Langley, 1969 —— 32 M358

"The aeronautical and space activities of the United States shall be conducted so as to contribute . . . to the expansion of human knowledge of phenomena in the atmosphere and space. The Administration shall provide for the widest practicable and appropriate dissemination of information concerning its activities and the results thereof."

— NATIONAL AERONAUTICS AND SPACE ACT OF 1958

NASA SCIENTIFIC AND TECHNICAL PUBLICATIONS

TECHNICAL REPORTS: Scientific and technical information considered important, complete, and a lasting contribution to existing knowledge.

TECHNICAL NOTES: Information less broad in scope but nevertheless of importance as a contribution to existing knowledge.

TECHNICAL MEMORANDUMS: Information receiving limited distribution because of preliminary data, security classification, or other reasons.

CONTRACTOR REPORTS: Scientific and technical information generated under a NASA contract or grant and considered an important contribution to existing knowledge.

TECHNICAL TRANSLATIONS: Information published in a foreign language considered to merit NASA distribution in English.

SPECIAL PUBLICATIONS: Information derived from or of value to NASA activities. Publications include conference proceedings, monographs, data compilations, handbooks, sourcebooks, and special bibliographies.

TECHNOLOGY UTILIZATION PUBLICATIONS: Information on technology used by NASA that may be of particular interest in commercial and other non-aerospace applications. Publications include Tech Briefs, Technology Utilization Reports and Notes, and Technology Surveys.

Details on the availability of these publications may be obtained from:

SCIENTIFIC AND TECHNICAL INFORMATION DIVISION

NATIONAL AERONAUTICS AND SPACE ADMINISTRATION

Washington, D.C. 20546